

Towards quantum state tomography of a single polariton state of an atomic ensemble

S.L. Christensen, J.B. Béguin, H.L. Sørensen, E. Bookjans,
D. Oblak, J.H. Müller, J. Appel and E.S. Polzik

QUANTOP, Niels Bohr Institute, University of Copenhagen, Blegdamsvej 17,
2100 Copenhagen, Denmark

E-mail: polzik@nbi.ku.dk

Abstract. We present a proposal and experimental progress towards quantum state tomography of a single polariton state of an atomic ensemble. The collective non-classical and non-Gaussian state of the ensemble is generated by detection of a single forward scattered photon. The state is subsequently characterized by atomic state tomography performed using strong dispersive light-atoms interaction followed by a homodyne measurement on the transmitted light. The proposal is backed by preliminary experimental results showing projection noise limited sensitivity and a simulation demonstrating the feasibility of the proposed method for detection of a non-classical and non-Gaussian state of the mesoscopic atomic ensemble. This work represents the first attempt of hybrid discrete-continuous variable quantum state processing with atomic ensembles.

PACS numbers: 03.65.Wj, 32.80.Qk, 42.50.Dv

1. Introduction

Atomic ensembles have emerged as a highly efficient medium for light-matter quantum interfaces [1]. Mapping of squeezed states of light onto an ensemble [2, 3], generation and retrieval of single excitations [4, 5, 6], entanglement of two ensembles [7, 8, 9] and quantum sensing [10, 11, 12] have all been demonstrated experimentally. The development of interfaces between light and atomic ensembles have so far followed two separate paths which until now have been pursued independently. Operating with either discrete excitations and single photon detection or with continuous Gaussian states and homodyne measurements. Within the latter approach tomography of spin squeezed atomic states by quantum non-demolition (QND) interactions with light has been developed [13, 14, 15].

In close analogy to methods used in photonic systems [16, 17], the hybrid approach of combining discrete excitations, such as number states, and measurements in the continuous variable domain opens up new venues in quantum state engineering with atomic ensembles. Among them are hybrid quantum repeaters and generation of Schrödinger cat states [18], weak quantum measurements [19] and heralded quantum amplification for precision measurements [20]. Also, preparing the quantum states of interest directly inside an atomic ensemble with a long coherence time, quantum-memory storage inefficiencies are avoided and the heralded state can be used on demand with a single mapping operation.

In the following, we report on the first steps towards bridging the gap between the discrete and continuous variable approaches with atomic ensembles. Starting from a collective photon scattering as in Duan et al.[21], we present a method to produce and directly characterize a highly non-classical (negative Wigner function) and non-Gaussian collective (entangled) atomic state. Using interference between different atomic spin-wave modes allows us to demonstrate its properties.

2. Generation of a single polariton state

We consider a system of N_a spin-1/2 particles described by the states $|\uparrow\rangle$ and $|\downarrow\rangle$ which in the experiment are the two hyperfine ground states of a Cesium (Cs) atom, also known as the clock-levels. Initially all atoms are prepared in the $|\uparrow\rangle$ state (figure 1a), such that the quantum state of the ensemble can be written as the product state

$$|\Psi_0\rangle = \bigotimes_{j=1}^{N_a} |\uparrow\rangle_j = |\uparrow\uparrow \dots \uparrow\uparrow\rangle. \quad (1)$$

Next, a weak off-resonant excitation pulse is sent into the ensemble, and conditioned on the detection of one photon scattered forward via a Raman process, one spin flip occurs in the collective polariton state of the ensemble. This detection event heralds the preparation of a single excitation of a collective atomic zero-transverse-momentum spin wave - a single polariton (figure 1b). The success probability of this forward scattering is kept low, such that the probability to forward-scatter two or more photons is negligible. The state of the ensemble [21] becomes

$$|\Psi_1\rangle = \hat{a}^\dagger |\Psi_0\rangle = \frac{1}{\sqrt{N_a}} \sum_{j=1}^{N_a} |\uparrow\uparrow \dots \uparrow \underbrace{\downarrow}_{j\text{-th atom}} \uparrow \dots \uparrow\rangle, \quad (2)$$

where we have defined the symmetric creation operator

$$\hat{a}^\dagger = \frac{1}{\sqrt{N_a}} \sum_{j=1}^{N_a} |\downarrow\rangle_j \langle \uparrow|_j. \quad (3)$$

To describe the atomic ensemble we define pseudo spin operators for each individual atom

$$\hat{j}_x \equiv \frac{1}{2} (|\downarrow\rangle \langle \uparrow| + |\uparrow\rangle \langle \downarrow|), \quad (4)$$

$$\hat{j}_y \equiv -\frac{i}{2} (|\downarrow\rangle \langle \uparrow| - |\uparrow\rangle \langle \downarrow|), \quad (5)$$

$$\hat{j}_z \equiv \frac{1}{2} (|\uparrow\rangle \langle \uparrow| - |\downarrow\rangle \langle \downarrow|), \quad (6)$$

which obey angular-momentum like commutation relations. From these we define symmetric (under particle exchange) collective ensemble operators by summing the individual atomic operators as

$$\hat{J}_i = \sum_{l=1}^{N_a} \hat{j}_i^{(l)} \quad \text{for } i = x, y, z. \quad (7)$$

where N_a is the total number of atoms in the ensemble and $\hat{j}_i^{(l)}$ acts on the l -th atom.

A subsequent microwave $\pi/2$ -pulse rotates this collective entangled state (figure 1c) such that it becomes an even superposition of $|\uparrow\rangle$ and $|\downarrow\rangle$ given as

$$|\Psi'_1\rangle = \hat{R}_{\pi/2} |\Psi_1\rangle \quad (8)$$

$$= \frac{1}{\sqrt{N_a}} \sum_{j=1}^{N_a} |+\dots+\underbrace{-}_{j\text{-th atom}}+\dots+\rangle, \quad (9)$$

where the microwave $\pi/2$ pulse is described by the operator

$$\hat{R}_{\pi/2} = \sum_{j=1}^{N_a} (|+\rangle_j \langle \uparrow|_j + |-\rangle_j \langle \downarrow|_j), \quad (10)$$

and the coherent superposition states are

$$|\pm\rangle \equiv \frac{|\uparrow\rangle \pm |\downarrow\rangle}{\sqrt{2}}. \quad (11)$$

To show that the state $|\Psi'_1\rangle$ has a non-Gaussian population-difference between the two hyperfine levels we calculate the probability to find n atoms in the $|\downarrow\rangle$ state and the remaining $N_a - n$ atoms in the $|\uparrow\rangle$ state. This is done by calculating the overlap between the single excitation state and the general n -th excited state given by

$$|\Psi_n\rangle = \binom{N_a}{n}^{-1/2} \sum_{\text{permutations}} | \underbrace{\uparrow}_{N_a - n} \underbrace{\downarrow}_n \rangle \quad (12)$$

we find

$$|\langle \Psi_n | \Psi'_1 \rangle|^2 = 2^{-N_a} \binom{N_a}{n} \frac{4}{N_a} \left(n - \frac{N_a}{2} \right)^2 \quad (13)$$

$$\stackrel{N_a \rightarrow \infty}{\approx} 2x^2 \sqrt{\frac{2}{\pi N_a}} e^{-x^2}, \quad (14)$$

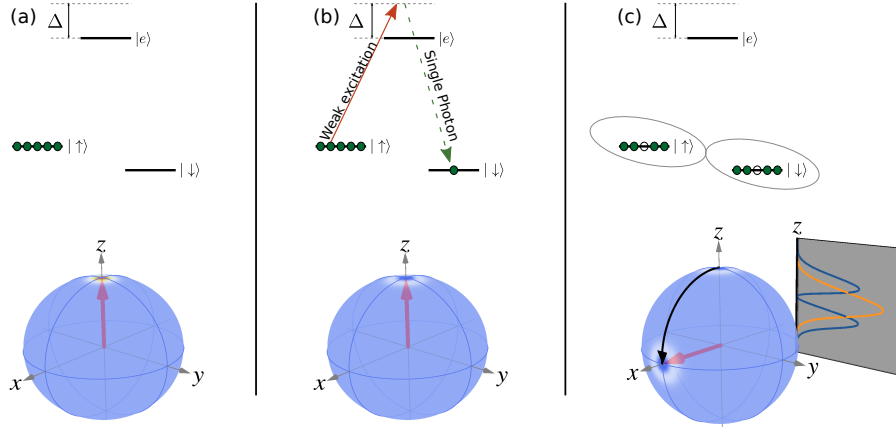


Figure 1. The atomic levels and Bloch spheres at different stages of the protocol (a) Atoms are prepared in $|\Psi_0\rangle$ and a weak blue detuned excitation pulse is applied (b) detection of a forward scattered Raman photon signals the generation of a single Fock state collective excitation in the ensemble (c) a microwave $\pi/2$ pulse rotates the state $|\Psi_1\rangle$ into the equatorial plane of the Bloch sphere, the insert shows a plot of the non-Gaussian (Gaussian) marginal distribution of the $|\Psi'_1\rangle$ ($|\Psi'_0\rangle$) state after a rotation to the equatorial plane in blue (orange).

whereas the standard coherent spin state (CSS) $|\Psi'_0\rangle$ has

$$|\langle \Psi_n | \Psi'_0 \rangle|^2 = 2^{-N_a} \binom{N_a}{n} \quad (15)$$

$$\stackrel{N_a \rightarrow \infty}{\approx} \sqrt{\frac{2}{\pi N_a}} e^{-x^2}, \quad (16)$$

with $x = \sqrt{\frac{2}{N_a}} (n - \frac{N_a}{2})$. From this it is clear that, *conditioned* on whether a single photon is detected or not, the probability distributions for outcomes of \hat{J}_y - and \hat{J}_z -measurements will be profoundly different, see insert on figure 1c.

In the ideal case of perfect tomography of a pure single polariton excitation the population difference follows the marginal distribution of a Wigner function with a single excitation, a $n = 1$ Fock-state, given by equation (14). In a realistic case of finite efficiency of both the state preparation and state detection we show that the marginal distribution still retains its non-classical and non-Gaussian features, as discussed in detail in section 3. Before we continue to the experimental implementation we introduce the effective quantum efficiency of the quadrature measurement, ϵ . This is equivalent to the efficiency of the state tomography which is based on the quadrature measurements. These are done with a dispersive QND-probing method introduced in [22] and discussed in detail in [14, 23]. It is performed with two probes, each of which interacts with the $|\uparrow\rangle$ ($|\downarrow\rangle$) state exclusively and which therefore does not cause Raman transitions to the other clock state $|\downarrow\rangle$ ($|\uparrow\rangle$). Each of these probes measures the atomic state dependent optical phase shift, which we then convert into quadrature values [24]. By a noise scaling analysis we discriminate light shot noise and technical noise against

the atomic noise. With this we quantify the efficiency as

$$\epsilon = \frac{\text{var}(\text{CSS}(N_a)) - \text{var}(\text{CSS}(N_a = 0))}{\text{var}(\text{CSS}(N_a))}. \quad (17)$$

Here $\text{CSS}(N_a)$ denotes the differential phase shift measured on a coherent spin state $|\Psi'_0\rangle$ with N_a atoms. Note that $\text{var}(\text{CSS}(N_a = 0))$ (the optical phase fluctuations measured in the absence of atoms) contains both shot noise and technical noise. The contribution of atomic noise to $\text{var}(\text{CSS}(N_a))$ scales quadratically with the number of photons in the probe, whereas the shot noise contribution only scales linearly [1]. For tomography applications it is not necessary to preserve the non-destructiveness of the QND probing – that is to preserve the coherence between the states $|\uparrow\rangle$ and $|\downarrow\rangle$. Therefore, neglecting technical noise, a probe of unlimited strength can in principle be used, and the quantum efficiency of the tomographic measurement will approach unity.

3. Implementation

As described in section 2, the Wigner function of the single polariton state has both a non-Gaussian marginal distribution and a negativity and is therefore highly non-classical. Over the past years several experiments have shown atomic state tomography [10, 13, 23, 25] in which the characterization of such a state could be performed. In the following we will present a detailed discussion on how a single polariton state can be created and characterized. We will focus on the specific experimental configuration described in [14, 23].

3.1. Experimental considerations

The experiment is based on an ensemble of approximately 10^5 Cs atoms. We consider the two-level system formed by the clock levels, i.e. $|\downarrow\rangle \equiv |F = 3, m_F = 0\rangle$ and $|\uparrow\rangle \equiv |F = 4, m_F = 0\rangle$. As the excited state, used to couple the two clock states, we use the $|e\rangle \equiv |F' = 4, m'_F = +1\rangle$ state of the 852 nm D2 transition. The atomic ensemble is situated in a far-off resonant dipole trap which is placed in one arm of a Mach-Zehnder interferometer (MZI), see figure 2. To obtain the probability distribution of \hat{J}_z -measurement outcomes, we detect the *atomic state dependent* optical phase-shift imprinted on light passing through the atomic ensemble using a dual-color dispersive QND measurement as described in section 2. To create the single polariton state given by equation (2) we propose the following procedure; initially all atoms are prepared in the $|\uparrow\rangle$ state by a combination of microwave pulses and optical pumping [26]. The collective excitation is created by a weak excitation pulse, blue detuned by $\Delta \approx \frac{3}{2}\Gamma$ from the $|\uparrow\rangle \rightarrow |e\rangle$ transition. The detuning is chosen such that the optical depth is less than unity, (assumed on resonant optical depth of $\text{OD} \approx 10$) which means that all atoms will have about the same chance to scatter a photon. If this condition is fulfilled the excitation will be collective, i.e. shared almost uniformly by the whole ensemble.

To obtain the best possible spatial overlap between the probe beams and the excitation beam with the atomic ensemble all beams arrive at the MZI input via the same optical fiber, whose output is carefully overlapped with the atomic sample. This nearly perfect overlap of the light beams obtained by using the same optical fiber comes with the constraint that the polarization of the excitation beam and the probe beams are now identical. With the quantization axis (defined by the magnetic bias-field) chosen orthogonal to the propagation direction of the beams, we can only address π -

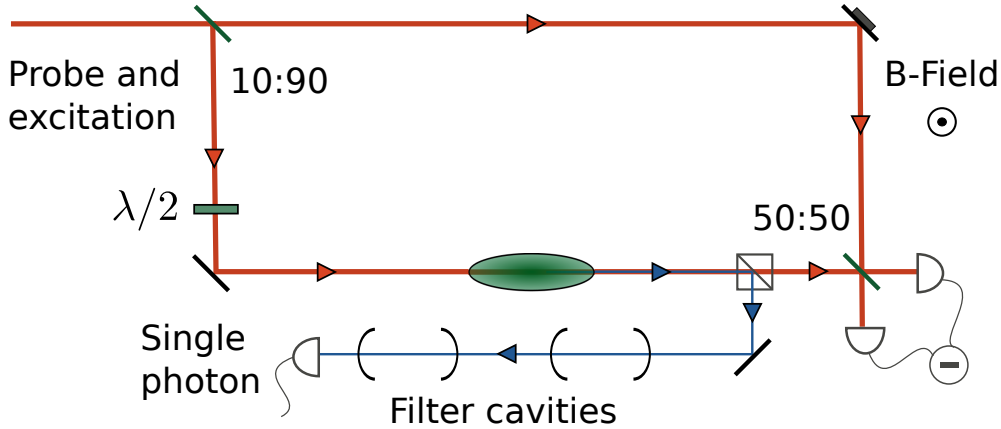


Figure 2. Sketch of the experimental setup. The atomic ensemble is trapped in a far off-resonant dipole trap (not shown). A single polariton state is generated by sending a weak excitation pulse through the atomic cloud. The detection of a forward scattered single photon heralds the creation of the desired state. Polarization and frequency filtering is applied to avoid the detection of undesired excitation photons using a polarizing beam splitter and two Fabry-Pérot filter cavities. To characterize the atomic state we measure the atomic state dependent optical phase shift imprinted on a light pulse by the atoms.

or x -polarized light. In order to obtain the highest efficiency of the atomic tomography it is preferable to use π -polarized light [14]. The complicated multi-level structure of the Cs atoms puts several constraints on the excitation and probe geometry and necessitates the application of a strong magnetic bias field as discussed in the following. Because of the symmetry of the $m_F = 0$ atomic wave functions, anti-Stokes photons on the Raman transition $|\uparrow\rangle \rightarrow |F' = 4\rangle \rightarrow |\downarrow\rangle$ cannot be emitted into the forward direction in the absence of an external magnetic field. In order to break the symmetry and to allow for forward Raman scattering into the $|\downarrow\rangle$ level a magnetic bias field is applied and the light polarization is adjusted to contain an x -component.

The applied bias field is approximately 20 Gauss which shifts the $|F' = 4, m'_F = -1\rangle$ out of resonance by several line widths, see figure 3. This choice combined with the fact that the $|\uparrow\rangle \rightarrow |F' = 4, m'_F = 0\rangle$ transition is forbidden by selection rules allows us to achieve the required selective excitation to the $|e\rangle$ state. From the $|e\rangle$ state the atom can undergo spontaneous emission through six possible decay channels, see figure 3.

We now apply different filtering methods such that we only detect photons corresponding to an atom decaying via the $|e\rangle \rightarrow |\downarrow\rangle$ transition, since this projects the ensemble into the single polariton state given by equation (2). Photons with π -polarization are suppressed by a polarizing beam splitter. The harder task is to filter out photons that are x -polarized and have a frequency corresponding to the $|e\rangle \rightarrow |F = 4\rangle$ manifold. Photons with these properties originate from both the excitation beam and the spontaneous decay. We thus need to reject photons with a frequency difference of approximately 9 GHz. We achieve this with two cascaded Fabry-Pérot filter cavities, see figure 2. This way we filter out all photons except the ones originating from the undesired decay channel $|e\rangle \rightarrow |F = 3, m_F = 2\rangle$. This decay channel produces forward scattered photons which have the same polarization

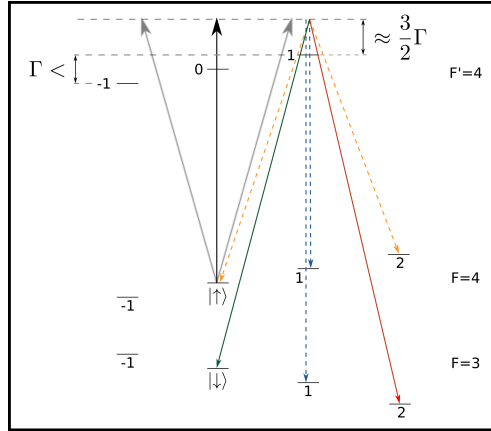


Figure 3. Cs level structure and excitation scheme: Upwards arrows indicate the excitation light and the downward arrows indicate decay channels. Light corresponding to the dashed arrows is filtered out by either polarization (blue) or frequency (orange). Solid arrows denote decays that *cannot* be filtered out. Note that the decay to $|F = 3, m_F = 2\rangle$ leads to the unavoidable inefficiency of the state generation as discussed in the text.

as the desired photon, the frequency difference between them is in the MHz range (the Zeeman splitting of the ground state), which makes it experimentally very hard to selectively reject them. Note that the branching ratios favor the preferred decay by a factor of ≈ 4 .

With the single photon detected, we proceed in a fashion similar to J. Appel et al. [23]. We apply a $\pi/2$ -pulse and perform the dispersive QND probing of the atomic population difference in $|\uparrow\rangle$ and $|\downarrow\rangle$. Repeating this procedure several thousand times we characterize the distribution of \hat{J}_z -measurements for the prepared atomic state. Note that due to the rotational symmetry of the Wigner function of both the single polariton- and the coherent spin-state the $\pi/2$ rotation can be performed without paying attention to the phase of the microwave pulse (which defines the axis of rotation on the Bloch sphere).

3.2. Test of tomography noise performance

The major experimental challenge is concerning the characterization of the atomic state via quantum tomography, since this requires the measurement of the population difference (\hat{J}_z) in the experimental apparatus to be projection noise limited. We have checked our noise sensitivity in the experimental configuration with a bias-field of $B \approx 20$ Gauss, corresponding to a splitting between the $|e\rangle$ and $|F' = 4, m'_F = -1\rangle$ states of several line widths.

We start by preparing a CSS of the atomic ensemble (a product state of each atom being in $|+\rangle$) [23] and then measure the population difference between the two clock-levels $|\uparrow\rangle$ and $|\downarrow\rangle$. Repeating this several thousands times and performing a noise scaling analysis, we attribute the measured fluctuations to different origins, see figure 4. We see a predominantly linear dependence of the atomic noise on the atom number – a clear signature of the required projection noise limited sensitivity. This certifies sufficient performance of the initial state preparation, the quality of our microwave

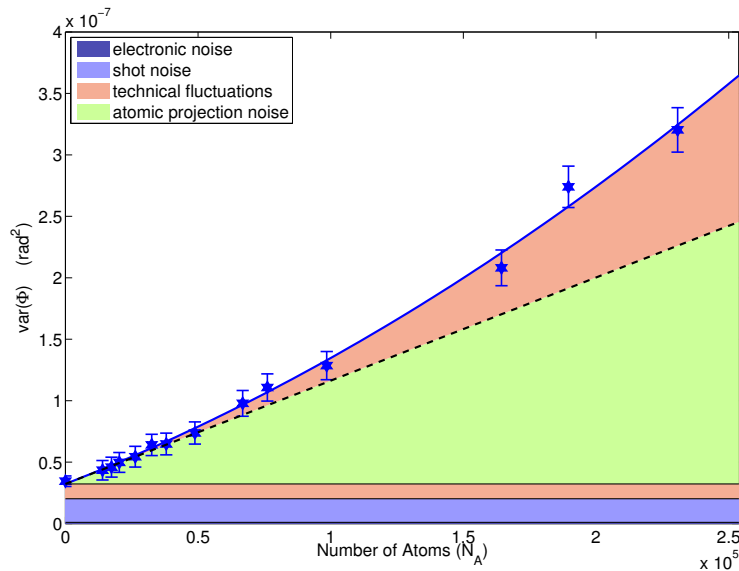


Figure 4. The measured variance of the probe phase as a function of atom number, with different noise contributions singled out via a noise scaling analysis.

source and the long term stability of our setup.

The next part of the experiment is to detect the single photon, distinguishing and filtering out photons originating from the excitation beam and undesired decay channels. Detection of any of these photons would result in false positive “clicks” i.e. we detect a photon but the atomic ensemble is not prepared in the desired single excitation state $|\Psi_1\rangle$. Such “clicks” could be due to dark counts, leakage of the probe-, trap- or excitation-beams. Since the state generation is based on the detection of a single photon with a low success probability, false positives essentially mix in realizations prepared in the vacuum state (zero polaritons).

To describe this, we consider the actual state prepared conditioned on a “click” as a classical mixture of the single excitation state $|\Psi'_1\rangle$ which is obtained with a probability p , and the CSS obtained with a probability $(1 - p)$:

$$\hat{\rho} = p |\Psi'_1\rangle \langle \Psi'_1| + (1 - p) |\Psi'_0\rangle \langle \Psi'_0| \quad (18)$$

In order to show that the outlined procedure is suitable for our experimental apparatus we perform an analysis based on a simulation using the relevant experimental parameters.

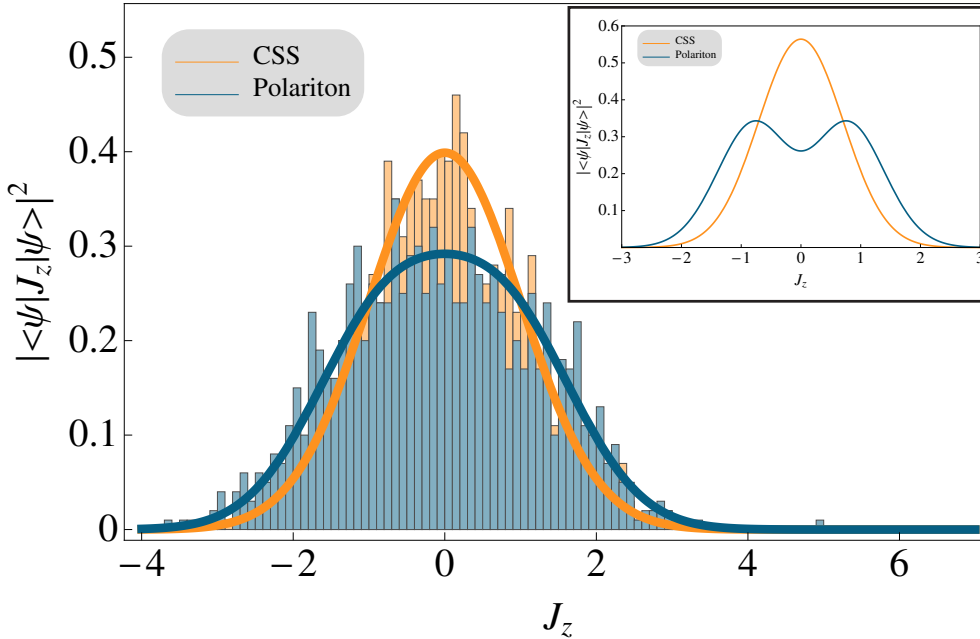
4. Analysis

To quantify the non-Gaussian character of the prepared state we calculate the expected probability distributions for our experimental parameters and perform a simulation similar to Dubost et al. [27].

In order to estimate the purity of the single polariton excitation (the probability p introduced in the previous section), we assume that the excitation pulse is so weak that the probability of producing a forward-scattered photon is 5%. To reach this scattering probability we require $1.35 \cdot 10^4$ photons in a $10 \mu\text{s}$ long excitation pulse.

Table 1. Probability for different origins of the photon giving rise to a click. We have only kept the most dominant processes, i.e. probabilities greater than 0.05 %.

Origin of photo-count	Created state	Probability (%)
Dark counts	$ \Psi_0\rangle$	8.7
Leakage of excitation pulse	$ \Psi_0\rangle$	0.6
Decay via $ e\rangle \rightarrow F = 3, m_F = 2\rangle$	$ \Psi_0\rangle$	19.1
Decay via $ e\rangle \rightarrow \downarrow\rangle$	$ \Psi_1\rangle$	71.5

**Figure 5.** Calculated distributions for J_z -measurements outcomes of the created single polariton state (blue) and the vacuum state (orange), taking into account the finite tomography efficiency. The histogram is based on 1000 randomly drawn samples from each distribution. Insert: Marginal distributions *not* including the effects of a non-unity detection efficiency. Note that the less-than-unity tomography efficiency washes away the non-Gaussian feature, making it hard to distinguish the two histograms by eye.

The polarization filtering is done with a polarizing beam splitter cube with a rejection of $1 : 7 \cdot 10^3$. For the frequency filtering we obtain rejections of $1 : 5 \cdot 10^7$ by using two cascaded filter cavities, each showing a transmission of 80 %. The mode-matching overlap of the single photon detection mode and the atomic state tomography mode is taken to be 75 %.

With this we estimate the probabilities of the photo-count originating from a specific decay channel, a dark count of the detector or from the leakage of other light sources (e.g. the excitation pulse) in the experiment. The probabilities of the dominating processes (those exceeding 0.05 %) are shown in table 1.

From the probability given in table 1 we calculate the probability distributions for J_z -measurements. The created state is modeled as a statistical mixture of a CSS and a

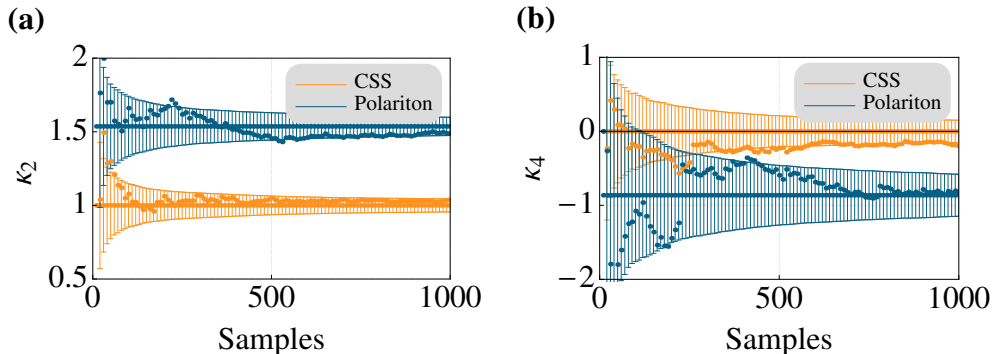


Figure 6. Plot of the cumulants as a function of the sample size. Dotted points is data from one realization simulation.

ideal, noise free single excitation state weighted with their corresponding probabilities, a plot is shown in the insert on figure 5. The efficiency of the atomic state tomography is reduced due to the extra noise added by the readout procedure: We use light as the meter-system and therefore the shot noise of light will also have a contribution. Following the approach outlined in [28] we model this independent Gaussian noise as an admixture of the vacuum state to the state to be analysed. In effect this reduces the non-Gaussianity of the \hat{J}_z distribution detected by the dispersive measurements as shown in the main panel of figure 5.

As pointed out in [27], the detection of a non-Gaussian marginal distribution is an experimental challenge. One of the main reasons for this is that we can only estimate the underlying probability distributions by a finite number of experimentally acquired samples. To illustrate this, we draw 1000 samples from the distributions for the dispersive \hat{J}_z measurements.

These samples are binned and plotted as a histogram in figure 5. It is clear from the histograms that distinguishing the two sets of sampled data and thus detecting the non-Gaussianity and possibly the non-classicality of the quantum state is experimentally challenging. Several methods have been developed in order to quantify the non-classicality [29, 30], note that the two papers do *not* use the same definition of non-classicality. Following the Vogel criterion for non-classicality the state given in equation (18) is non-classical for any p , as shown by Lvovsky et al. [31].

In the following we present a simulation based on the ideas in [27] where the non-Gaussianity is quantified in terms of the statistical cumulants. From the known probability distributions we draw random samples and use these to calculate the second and fourth cumulants, $\kappa_2 = \mu_2$ and $\kappa_4 = \mu_4 - 3\mu_2^2$, for varying sample sizes, μ_i denotes the i -th statistical moment. Repeating this 1000 times allows us to calculate the corresponding standard deviations, see figure 6. We start by considering the second order cumulant, which is just the variance of the distribution: From figure 6a we note that only around 250 samples are needed to distinguish between the distribution of the

single polariton state and the vacuum (CSS). We thus expect that careful investigation of κ_2 will allow us to clearly classify our data as originating from either the expected single polariton state or the CSS under the assumptions that these are the only possible distributions. In order to verify that our state is non-Gaussian we need to observe a non-zero fourth cumulant κ_4 . We expect to require approximately 500 samples to clearly distinguish the observed probability distribution from the Gaussian one of the CSS with $\kappa_4 = 0$. The performed simulations are based on realistic parameters, many already experimentally verified, and we can thus conclude that our proposed implementation is experimentally feasible.

5. Conclusion

In this paper we have introduced a hybrid method based on discrete excitations and continuous measurements which allows us to generate and characterize a single polariton state of an atomic ensemble. This state has non-Gaussian marginal distributions of the Wigner function and is non-classical. We have presented a detailed proposal for the experimental creation and detection of the single polariton state. The proposal is backed by a simulation for experimental valid parameters together with preliminary results showing the feasibility of the proposal. This work is a step towards implementing a hybrid approach to quantum information processing with atomic memories as well as a contribution to the ongoing research into the foundations of quantum mechanics.

Acknowledgments

We thank A. Sørensen and E. Kot for helpful discussions regarding the state preparation and quantification of non-classicality and A. Louchet-Chauvet, J. J. Renema, and N. Kjærgaard for contributions in the earlier stages of the experiment. The presented work has been supported by the Danish National Research Foundation, DARPA project QUASAR, and EU project Q-ESSENCE.

References

- [1] K. Hammerer, A. Sørensen, and E. Polzik. “Quantum interface between light and atomic ensembles”. *Reviews Of Modern Physics* **82** (Apr. 2010), p. 1041. DOI: [10.1103/RevModPhys.82.1041](https://doi.org/10.1103/RevModPhys.82.1041).
- [2] N. P. Georgiades, E. S. Polzik, K. Edamatsu, H. J. Kimble, and A. S. Parkins. “Nonclassical excitation for atoms in a squeezed vacuum”. *Physical Review Letters* **75** (Nov. 1995), pp. 3426–3429. DOI: [10.1103/PhysRevLett.75.3426](https://doi.org/10.1103/PhysRevLett.75.3426).
- [3] J. Hald, J. L. Sørensen, C. Schori, and E. S. Polzik. “Spin squeezed atoms: a macroscopic entangled ensemble created by light”. *Physical Review Letters* **83**.7 (Aug. 1999), pp. 1319–1322. DOI: [10.1103/PhysRevLett.83.1319](https://doi.org/10.1103/PhysRevLett.83.1319).
- [4] M. D. Lukin. “Colloquium: trapping and manipulating photon states in atomic ensembles”. *Reviews of Modern Physics* **75** (Apr. 2003), pp. 457–472. DOI: [10.1103/RevModPhys.75.457](https://doi.org/10.1103/RevModPhys.75.457).

- [5] K. S. Choi, H. Deng, J. Laurat, and H. J. Kimble. “Mapping photonic entanglement into and out of a quantum memory”. *Nature* **452** (Mar. 2008), pp. 67–71. DOI: [10.1038/nature06670](https://doi.org/10.1038/nature06670).
- [6] M. Albert, A. Dantan, and M. Drewsen. “Cavity electromagnetically induced transparency and all-optical switching using ion Coulomb crystals”. *Nature Photonics* **5** (Oct. 2011), pp. 633–636. DOI: [10.1038/nphoton.2011.214](https://doi.org/10.1038/nphoton.2011.214).
- [7] B. Julsgaard, A. Kozhokin, and E. S. Polzik. “Experimental long-lived entanglement of two macroscopic objects”. *Nature* **413** (Sept. 2001), pp. 400–403. DOI: [10.1038/35096524](https://doi.org/10.1038/35096524).
- [8] H. Krauter, C. A. Muschik, K. Jensen, W. Wasilewski, J. M. Petersen, J. I. Cirac, and E. S. Polzik. “Entanglement generated by dissipation and steady state entanglement of two macroscopic objects”. *Physical Review Letters* **107.8** (Aug. 2011), pp. 080503–+. DOI: [10.1103/PhysRevLett.107.080503](https://doi.org/10.1103/PhysRevLett.107.080503).
- [9] C. W. Chou, H. de Riedmatten, D. Felinto, S. V. Polyakov, S. J. van Enk, and H. J. Kimble. “Measurement-induced entanglement for excitation stored in remote atomic ensembles”. *Nature* **438** (Dec. 2005), pp. 828–832. DOI: [10.1038/nature04353](https://doi.org/10.1038/nature04353).
- [10] I. D. Leroux, M. H. Schleier-Smith, and V. Vuletić. “Orientation-dependent entanglement lifetime in a squeezed atomic clock”. *Physical Review Letters* **104.25**, 250801 (June 2010), p. 250801. DOI: [10.1103/PhysRevLett.104.250801](https://doi.org/10.1103/PhysRevLett.104.250801).
- [11] M. Napolitano, M. Koschorreck, B. Dubost, N. Behbood, R. J. Sewell, and M. W. Mitchell. “Interaction-based quantum metrology showing scaling beyond the Heisenberg limit”. *Nature* **471** (Mar. 2011), pp. 486–489. DOI: [10.1038/nature09778](https://doi.org/10.1038/nature09778).
- [12] W. Wasilewski, K. Jensen, H. Krauter, J. J. Renema, M. V. Balabas, and E. S. Polzik. “Quantum noise limited and entanglement-assisted magnetometry”. *Physical Review Letters* **104.13** (Apr. 2010), pp. 133601–+. DOI: [10.1103/PhysRevLett.104.133601](https://doi.org/10.1103/PhysRevLett.104.133601).
- [13] T. Fernholz, H. Krauter, K. Jensen, J. F. Sherson, A. S. Sørensen, and E. S. Polzik. “Spin squeezing of atomic ensembles via nuclear-electronic spin entanglement”. *Physical Review Letters* **101.7**, 073601 (Aug. 2008), p. 073601. DOI: [10.1103/PhysRevLett.101.073601](https://doi.org/10.1103/PhysRevLett.101.073601).
- [14] A. Louchet-Chauvet, J. Appel, J. J. Renema, D. Oblak, N. Kjærgaard, and E. S. Polzik. “Entanglement-assisted atomic clock beyond the projection noise limit”. *New Journal Of Physics* **12.6** (June 2010), pp. 065032–+. DOI: [10.1088/1367-2630/12/6/065032](https://doi.org/10.1088/1367-2630/12/6/065032).
- [15] T. Takano, M. Fuyama, R. Namiki, and Y. Takahashi. “Spin squeezing of a cold atomic ensemble with the nuclear spin of one-half”. *Phys. Rev. Lett.* **102.3**, 033601 (Jan. 2009), p. 033601. DOI: [10.1103/PhysRevLett.102.033601](https://doi.org/10.1103/PhysRevLett.102.033601).

- [16] A. Ourjoumtsev, H. Jeong, R. Tualle-Brouiri, and P. Grangier. “Generation of optical Schrödinger cats from photon number states”. *Nature* **448** (Aug. 2007), pp. 784–786. DOI: [10.1038/nature06054](https://doi.org/10.1038/nature06054).
- [17] J. S. Neergaard-Nielsen, B. M. Nielsen, C. Hettich, K. Molmer, and E. S. Polzik. “Generation of a superposition of odd photon number states for quantum information networks”. *Physical Review Letters* **97.8**, 083604 (Aug. 2006), p. 083604. DOI: [10.1103/PhysRevLett.97.083604](https://doi.org/10.1103/PhysRevLett.97.083604).
- [18] J. B. Brask, I. Rigas, E. S. Polzik, U. L. Andersen, and A. S. Sørensen. “Hybrid long-distance entanglement distribution protocol”. *Physical Review Letters* **105.16** (Oct. 2010), pp. 160501–+. DOI: [10.1103/PhysRevLett.105.160501](https://doi.org/10.1103/PhysRevLett.105.160501).
- [19] C. Simon and E. S. Polzik. “Fock-state view of weak-value measurements and implementation with photons and atomic ensembles”. *Phys. Rev. A* **83.4**, 040101 (Apr. 2011), p. 040101. DOI: [10.1103/PhysRevA.83.040101](https://doi.org/10.1103/PhysRevA.83.040101).
- [20] N. Brunner, E. S. Polzik, and C. Simon. “Heralded amplification for precision measurements with spin ensembles”. *Phys. Rev. A* **84** (4 Oct. 2011), p. 041804. DOI: [10.1103/PhysRevA.84.041804](https://doi.org/10.1103/PhysRevA.84.041804).
- [21] L. M. Duan, M. D. Lukin, J. I. Cirac, and P. Zoller. “Long-distance quantum communication with atomic ensembles and linear optics”. *Nature* **414** (6862 Nov. 2001), pp. 413–18. ISSN: 0028–0836. DOI: [10.1038/35106500](https://doi.org/10.1038/35106500).
- [22] M. Saffman, D. Oblak, J. Appel, and E. S. Polzik. “Spin squeezing of atomic ensembles by multicolor quantum nondemolition measurements”. *Physical Review A* **79.2** (Feb. 2009), pp. 023831–+. DOI: [10.1103/PhysRevA.79.023831](https://doi.org/10.1103/PhysRevA.79.023831).
- [23] J. Appel, P. J. Windpassinger, D. Oblak, U. Busk Hoff, N. Kjærgaard, and E. S. Polzik. “Mesoscopic atomic entanglement for precision measurements beyond the standard quantum limit”. *Proceedings Of The National Academy Of Sciences* **106** (June 2009), pp. 10960–10965. DOI: [10.1073/pnas.0901550106](https://doi.org/10.1073/pnas.0901550106).
- [24] T. Kiesel, W. Vogel, S. L. Christensen, J.-B. Béguin, J. Appel, and E. S. Polzik. “Atomic nonclassicality quasiprobabilities”. *ArXiv e-prints* (July 2012). arXiv:[1207.3314](https://arxiv.org/abs/1207.3314) [quant-ph].
- [25] R. Schmied and P. Treutlein. “Tomographic reconstruction of the Wigner function on the Bloch sphere”. *New Journal of Physics* **13.6** (June 2011), p. 065019. DOI: [10.1088/1367-2630/13/6/065019](https://doi.org/10.1088/1367-2630/13/6/065019).
- [26] P. J. Windpassinger, D. Oblak, U. Busk Hoff, J. Appel, N. Kjærgaard, and E. S. Polzik. “Inhomogeneous light shift effects on atomic quantum state evolution in non-destructive measurements”. *New Journal Of Physics* **10.5** (May 2008), pp. 053032–+. DOI: [10.1088/1367-2630/10/5/053032](https://doi.org/10.1088/1367-2630/10/5/053032).
- [27] B. Dubost, M. Koschorreck, M. Napolitano, N. Behbood, R. J. Sewell, and M. W. Mitchell. “Efficient quantification of non-Gaussian spin distributions”. *Physical Review Letters* **108.18**, 183602 (May 2012), p. 183602. DOI: [10.1103/PhysRevLett.108.183602](https://doi.org/10.1103/PhysRevLett.108.183602).

- [28] J. Appel, D. Hoffman, E. Figueroa, and A. I. Lvovsky. “Electronic noise in optical homodyne tomography”. *Physical Review A* **75** (Mar. 2007), pp. 035802–+. DOI: [10.1103/PhysRevA.75.035802](https://doi.org/10.1103/PhysRevA.75.035802).
- [29] E. Kot, N. Grønbech-Jensen, B. M. Nielsen, J. S. Neergaard-Nielsen, E. S. Polzik, and A. S. Sørensen. “Breakdown of the classical description of a local system”. *Physical Review Letters* **108.23**, 233601 (June 2012), p. 233601. DOI: [10.1103/PhysRevLett.108.233601](https://doi.org/10.1103/PhysRevLett.108.233601).
- [30] W. Vogel. “Nonclassical states: an observable criterion”. *Physical Review Letters* **84** (Feb. 2000), pp. 1849–1852. DOI: [10.1103/PhysRevLett.84.1849](https://doi.org/10.1103/PhysRevLett.84.1849).
- [31] A. I. Lvovsky and J. H. Shapiro. “Nonclassical character of statistical mixtures of the single-photon and vacuum optical states”. *Phys. Rev. A* **65.3**, 033830 (Mar. 2002), p. 033830. DOI: [10.1103/PhysRevA.65.033830](https://doi.org/10.1103/PhysRevA.65.033830).